Solid State Communications 250 (2017) 41–44

Contents lists available at ScienceDirect

Solid State Communications

journal homepage: www.elsevier.com/locate/ssc

Communication

Twin grain boundary mediated ferromagnetic coupling in Co-doped ZnO: First-principles calculations

Jingjing Wu[a,b], Xin Tang[a,b,*], Chunying Pu[c], Fei Long[a,b], Biyu Tang[d]

[a] Key Lab of New Processing Technology for Nonferrous Metal & Materials, Ministry of Education, Guilin University of Technology, Guilin 541004, China
[b] College of Material Science and Engineering, Guilin University of Technology, Guilin 541004, China
[c] College of Physics and Electronics Engineering, Nan Yang Normal University, Nanyang 473061, China
[d] Department of Physics, Xiangtan University, Hunan Province, 411105, China

ARTICLE INFO

Keywords:
A. Dilute magnetic semiconductor
C. Twin grain boundary
E. First principle calculation

ABSTRACT

First principle calculation, based on density functional theory, is applied to study the electronic and magnetic properties of Co-doped ZnO $\sum 7$ $(12\bar{3}0)$ twin grain boundary. Co atoms substituting Zn at the threefold-coordination sites have the lowest formation energy, compared with other sites. More importantly, the configuration can result in the stable formation of ferromagnetic state (FM). Meanwhile, the strong Co-Co interaction is found to be responsible for the ferromagnetic state. Due to the structural character of the twin grain boundary, periodical defects can be offered, which favors the macroscopic FM ordering. The result also gives us a new thinking to understand the origin of FM in transition metal doped ZnO.

1. Introduction

Since Coey et al. theoretically predicted that a high Curie temperature (T_C) could be achieved in dilute magnetic semiconductor (DMS) based on wide-bandgap semiconductor, more attention has been paid to ZnO-based DMS, which has a direct wide band gap of 3.37 eV at room temperature [1]. In the past fifteen years, the prediction has been turned into reality. A giant amount of research show that the room temperature ferromagnetism (RTFM) can be found in ZnO doped with transition metal (TM) impurities such as Co, Mn, Cr, Cu, Fe, Ni and V [2–6]. In theory, many experimental results suggest that a carrier-mediated mechanism is not a feasible explanation for the origin of RTFM in some cases [7–9]. Instead, the structural defects play a key role, and the defects such as O vacancy (V_O) and Zn interstitial (Zn_i) are corresponding to the appearance of RTFM. Hong et al. found that the magnetic moment of the Cr-doped ZnO film reduced to be one order smaller after annealing, and the film crystallization was clearly improved in the same time [10,11]. Further analysis showed that the filling up of V_O might account for the decreasing magnetic moment. Similarly, Judith et al. reported that a short and low temperature anneal of Co-doped ZnO resulted in a decrease of the '*c*' lattice parameter caused by the Zn_i concentration, which was responsible for the decrease of RTFM [12].

In the ZnO film growth, V_O and Zn_i are the main defects. However, besides the two kinds of point defects, there are many other planar defects. In a sense, these 2D defects could be seen as the accumulation of point defects, and effect on the magnetic property in the TM-doped ZnO film. Straumal et al. researched the influence of the grain boundary (GB) on the appearance of FM in Co-doped ZnO and concluded that FM could be achieved if it contained enough GBs [13–15]. Generally, GB has a complicated structure and is difficult for constructing. However, twin grain boundary is an exception due to its high symmetry. In fact, HRTEM results have shown that $\sum 7$ $(12\bar{3}0)$ GB, a kind of twin grain boundary, really exist in ZnO film growth [16]. Recent calculation also predicted that the formation energy of the GB was 1.21 J/m^2 [17]. Since $\sum 7$ $(12\bar{3}0)$ GB is a kind of 2D structural defect, it should have an influence on FM in Co-doped ZnO. In this paper, first-principle calculation is applied to study the electronic and magnetic properties of Co-doped ZnO $\sum 7$ $(12\bar{3}0)$ twin grain boundary.

2. Method of calculation

The calculations have been performed in the framework of DFT with the projected augmented wave method [18], using the Vienna *ab initio* simulation package (VASP) [19]. For the exchange-correlation functional, a generalized gradient approximation (GGA) [20] in the form of Perdew-Burke-Ernzerhof (PBE) is employed. A Hubbard U term is also considered in the description of the electron-electron interaction in the 3d orbital [21]. In GGA+U, the Coulomb parameter U is set to 2.8 eV for Co and a typical value of J=1.0 eV is used for the

* Corresponding author at: College of Material Science and Engineering, Guilin University of Technology, Guilin 541004, China.
E-mail address: xtang@glut.edu.cn (X. Tang).

http://dx.doi.org/10.1016/j.ssc.2016.11.008
Received 17 August 2016; Received in revised form 5 November 2016; Accepted 10 November 2016
Available online 12 November 2016
0038-1098/

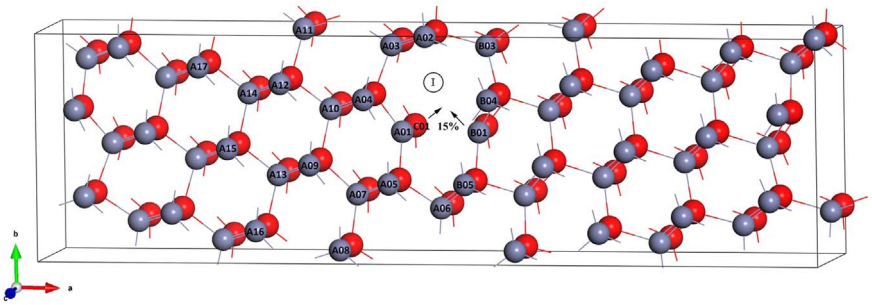

Fig. 1. The relaxed supercell of ZnO ∑7 (12$\bar{3}$0) GB. Light blue and red spheres designate Zn and O atoms, respectively. (For interpretation of the references to color in this figure legend, the reader is referred to the web version of this article)

exchange parameter [22]. For Zn, the values of 7.0 and 0.0 eV are adopted for U and J [23], respectively, because of the deeper and more localized d^{10} shell. A 112-host-atom supercell is used, as shown in Fig. 1. The plane-wave energy cutoff is set to 400 eV and the Γ-point centered 1×3×5 and 3×5×7 *k*-point mesh were used for atomic force relaxation and electronic structure analysis, respectively. The formation energy of a defect α is defined as

$$E_f(\alpha) = E(\alpha) - E(\text{host}) + \sum_i n_i \times E(i) \quad (1)$$

where $E(\alpha)$ and E(host) are the total energy of the host supercell containing ∑7 (12$\bar{3}$0) GBs with and without defects. n_i indicates the number of atoms of type i (host atoms or impurity atoms) that have been added to (n_i <0) or removed from (n_i >0) the supercell. The calculated E(Zn) and E(Co) are −1.12 and −4.30 eV, respectively, close to the experimental values [24].

3. Result and discussion

The relaxed configuration of ZnO ∑7 (12$\bar{3}$0) GB is shown in Fig. 1. Two antiparallel GBs are included in one supercell. In each GB unit, there are four threefold-coordination atoms, including two Zn and two O atoms, which are displaced inward by −15% due to the existence of the dangling bonds, as marked in Fig. 1. Moreover, there are large open channels along the GB plane, which could favor the formation and diffusion of interstitial atoms. The calculated formation energy is 1.25 J/m^2, close to the other theoretical calculation, 1.21 and 1.69 J/m^2 [17,25].

The electronic structure of the ZnO ∑7 (12$\bar{3}$0) GB is shown in Fig. 2a. According to the computed band structure for the GB, the predicted band gap is 1.65 eV, far below the experimental value of 3.37 eV, but the value agrees with the other GGA+U results [17]. The density of state (DOS) shows that a localized full-occupied band in the band gap origins from the $2p_x$ orbit of the O atoms with threefold-coordination, as shown in Fig. 2c. The band mainly composes of nonbonding electrons and leads to the formation of dangling bonds, which may promote the formation of FM.

There are 17 inequivalent sites for Co_{Zn} in the supercell and all of the positions have been labeled from A01 to A17, in Fig. 1. Based on Eq. (1), the formation energy of the 17 inequivalent Co_{Zn} is calculated, and the result is presented in Fig. 3a. We also calculated the formation energy of Co_i, Co atom at the interstitial site I. The calculated magnetic moments of configurations with Co at different sites are same, with the value of 3 μ_B/Co. For Co_i, although GB channel is large enough to accommodate one Cd atom, Co_i has the highest formation energy of −0.10 eV. Co_i only bonds with the two surrounding O atoms, which is less than the other Co_{Zn} with three or four O atoms. For Co_{Zn}, the smallest formation energy is −0.63 eV when Co_{Zn} at A01. Compared with Zn at this site, the distribution of the electrons coincides with that of Co atom, as showed in Fig. 2b. Co has a stronger hybridization with O. In addition, Co_{Zn} in A01 is a threefold-coordination, which can effectively relax the strain induced by Co_{Zn}.

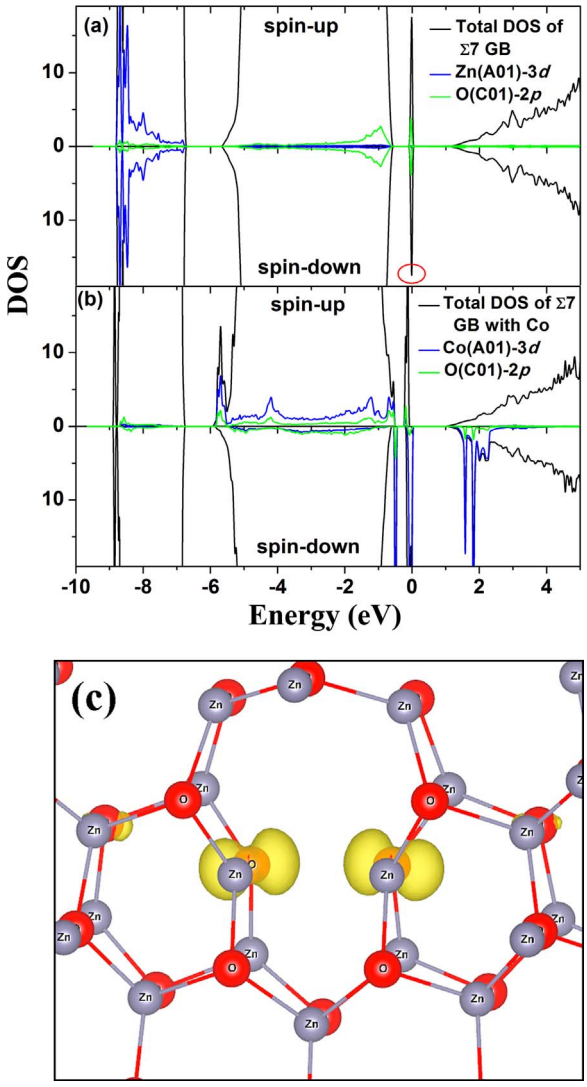

Fig. 2. (a) Calculated DOS of ZnO ∑7 (12$\bar{3}$0) GB without (a) and with (b) Co_{Zn} at site A01. Fermi level is set as the zero of energy. PDOS of Co and O is amplified to plot for clarity. (c) The isosurface (0.015 e/Å^3) of charge density of the localized energy band which has been circled in (a).

In order to investigate the mechanism of FM, the case of two Co_{Zn} in the supercell is discussed. There are more than 150 inequivalent configuration of two Co_{Zn} in the supercell. Since Co_{Zn} at A01 is most stable, more attention is paid to the site. Eleven possible configurations with FM and AFM ordering are calculated and the results are shown in Fig. 3b. As expected, A01-B01 (two Co_{Zn} at site A01and B01, respectively) has the lowest formation energy, with the value of −1.19 eV in FM state. The negative value also suggests that the

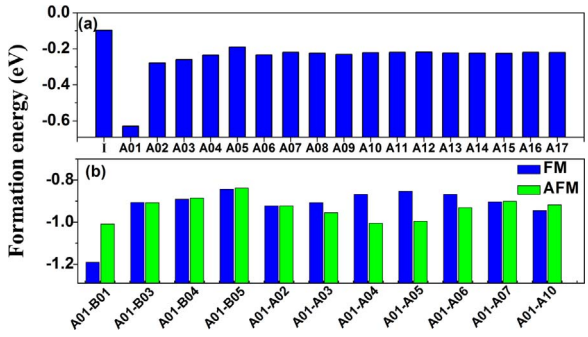

Fig. 3. The formation energies of Co_{Zn} at different sites (a) and the different configurations in FM and AFM state (b).

configuration is energetically favorable. More importantly, the formation of A01-B01 in FM state is 0.18 eV lower than that in AFM state, and the twin GB can induce the FM coupling between the two nearest-neighbor (NN) Co ions without the existence of point defects, such as V_O and Zn_i. The result is consistent with the Straumal's experiments, which found GBs are responsible for FM behavior in Co-doped ZnO [13–15]. Fig. 4a is the calculated total DOS result of the A01-B01 configuration in FM and AFM state. For the FM state, the main asymmetry distribution between spin-up and spin-down state is the discrete electron density distribution near the Fermi level. The Fermi level locates in the band gap, lower than the conduction band minimum, which also means that the carriers are not necessary for FM in this case. The discrete peaks mainly compose of O 2*p* and Co 3*d* orbital. Considering the symmetry of the GB, we only plot the partial density of state (PDOS) of Co_{Zn} at A01 and O atom at C01, as shown in Figs. 4b and c. The distribution does not accord with the usual tetrahedral crystal field splitting and is quite different from the electron density distribution of the general fourfold-coordination Co_{Zn} [26] or Co_{Zn}-V_O complex [27]. It is easy to understand, since the site A01 and C01 are not the center of tetrahedral. Co and three surrounding O atoms construct a nonstandard triangular pyramid, and the symmetry is broken. The energy level splitting of Co 3*d* orbital and the hybridization with O 2*p* orbital become complicated. However, PDOS analysis indicates that Co-Co interaction is stronger in FM than in AFM, which is mainly reflected in the part of spin down. For the spin down of FM, energy level splitting can be found and some discrete energy levels distribute from −1.5 to 0.0 eV. Some of the discrete energy levels only include Co 3*d* orbital. We choose an energy level occupied by Co *dxy* orbital, as labeled in Fig. 4b, and plot its partial charge density in Fig. 4d. The charge density has a character of a *d*-*d* π bond between the two Co atoms, which confirms the existence of the Co-Co interaction. It is reasonable that energy level splitting happens. On the contrary, for the case of AFM, most electrons occupy the band close to the Fermi level and no obvious energy level splitting is found. Moreover, the relaxed atomic structures show that the Co-Co bond length is 2.36 and 2.64 Å for FM and AFM state, respectively, while the value is only 2.50 Å for the hcp Co metal. The short bond length in FM state also demonstrates a strong Co-Co coupling and energy level splitting. As a result, the distribution of electrons to shifts to the low energy region and the formation of the A01-B01 configuration is effectively lowered.

Although the Co-Co dimer locally couples ferromagnetically, the inter-dimer coupling is the key to achieve the macroscopic FM ordering. Therefore, we further calculated the magnetic coupling between the Co-Co dimers with 5.1 Å along *c* axis, using a supercell containing 224 atoms, which has double size of the supercell used in Fig. 1. The result shows that FM is more stable by about 41 meV than AFM ordering. This energy difference is sufficient to stabilize FM against thermal fluctuations, since 30 meV is the minimum required to establish ferromagnetic coupling at RT [28]. Fig. 5 also shows the isosurface of the spin density distribution of the two Co-Co dimers in

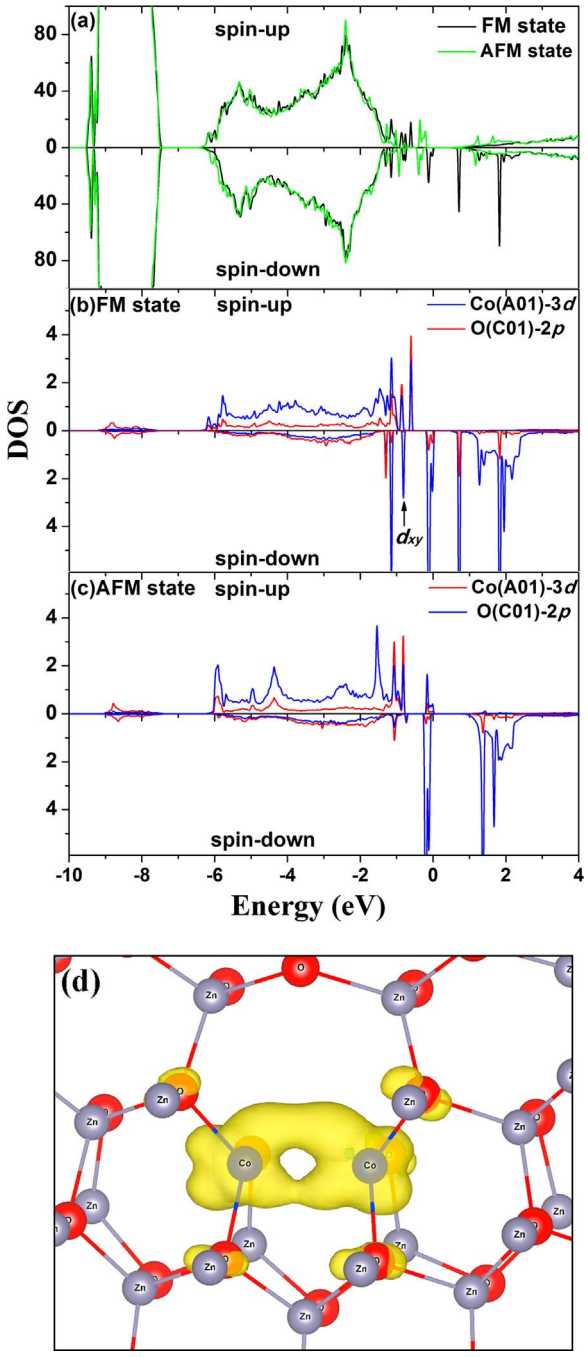

Fig. 4. (a) Calculated total DOS of the A01-B01 configuration in FM and AFM state. Partial DOS of Co and O atoms at site A01 and C01, respectively, in FM (b) and AFM (c) state. (d) The isosurface (0.003 $e/Å^3$) of charge density of the localized energy level which has been marked in (b).

the supercell. Besides the Co atoms, the electrons of the surrounding O atoms are also spin-polarized and the distribution of the spin-polarized electrons covers the whole period along *c* axis.

Based on the results obtained, we propose a model on the FM ordering mediated by twin GBs in Co-doped ZnO. Generally, twin GBs favor the formation of Co_{Zn}, as shown in Fig. 3a, which can lead to the aggregation of Co_{Zn} or Co-Co dimers in GBs. Due to the continuity of twin GB, the Co-Co dimers appears with a period of 5.10 and 8.45 Å along *c* and *b* axis, respectively. A percolative dimer mesh will form, and the macroscopic FM ordering is expected. The dimers can be intercoupling without the presence of carriers, which is different from the traditional carrier-mediated exchange mechanism [29]. The result

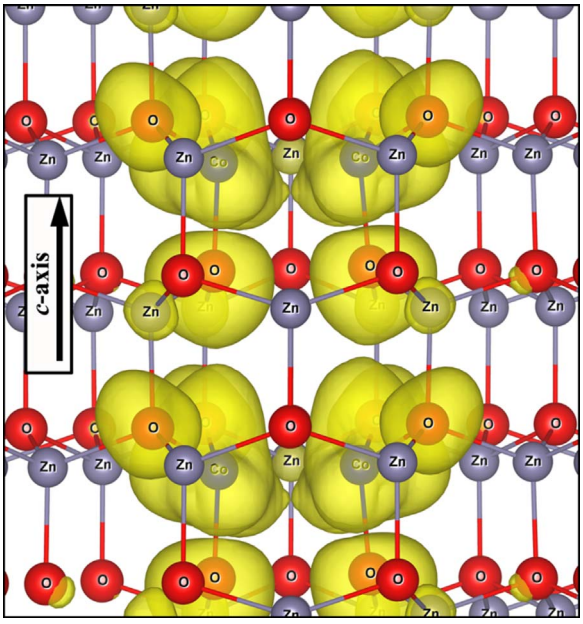

Fig. 5. The isosurface (0.001 $e/Å^3$) of the spin density distribution of the supercell which contains two Co-Co dimers.

proves that the carriers are not necessary for the formation of the FM ordering. In fact, many experiments have observed the FM in insulating Co-doped ZnO films [30–32]. In addition, the twin GB is a kind of 2D defect and has the characteristics of anisotropy. When the Co-Co dimers distribute in the twin GBs, the FM behavior should be anisotropic, which also agree with some experimental results [33]. ZnO $\sum 7\ (12\bar{3}0)$ GB is a special case of the twin GBs, but it gives us a new view to think the origin of FM ordering. Compared with point defects, twin GBs have periodic structural defects, relaxes the strain induced by transition metal doping, and also can mediate the FM coupling. The advantages make twin GBs become the potential candidate of the FM origin.

4. Conclusion

In summary, we present extensive theoretical calculation of the magnetic properties of Co-doped ZnO $\sum 7\ (12\bar{3}0)$ GB. We find that the energy of Co substituting Zn at the threefold-coordination site is lowest, rather than at the interstitial site. The FM ordering is energetically the most preferred state, when the Co-Co dimer forms with Co_{Zn} at site A01and B01. In the dimer, besides the Co atoms, the electrons of the surrounding O atoms are also spin-polarized, which results in the formation of the macroscopic FM ordering. Due to the structural character of 2D defects, the twin GBs facilitate the formation of FM and should be considered as an origin of FM ordering in TM-doped ZnO.

Acknowledgement

The work is supported by the National Natural Science Foundation of China under Grant No's. 11364009 and 10904021, and Natural Science Foundation of Guangxi Province (No. 2014GXNSFFA118004).

References

[1] J.M. Coey, M. Venkatesan, C.B. Fitzgerald, Nat. Mater. 4 (2005) 173–179.
[2] S.-W. Lim, D.-K. Hwang, J.-M. Myoung, Solid State Commun. 125 (2003) 231–235.
[3] Z. Yin, N. Chen, F. Yang, S. Song, C. Chai, J. Zhong, H. Qian, K. Ibrahim, Solid State Commun. 135 (2005) 430–433.
[4] L. Li, H. Liu, X. Luo, X. Zhang, W. Wang, Y. Cheng, Q. Song, Solid State Commun. 146 (2008) 420–424.
[5] J.H. Yang, Y. Cheng, Y. Liu, X. Ding, Y.X. Wang, Y.J. Zhang, H.L. Liu, Solid State Commun. 149 (2009) 1164–1167.
[6] Z.H. Wang, D.Y. Geng, Z.D. Zhang, Solid State Commun. 149 (2009) 682–684.
[7] F. Pan, C. Song, X.J. Liu, Y.C. Yang, F. Zeng, Mater. Sci. Eng.: R: Rep. 62 (2008) 1–35.
[8] S. Mal, J. Narayan, S. Nori, J.T. Prater, D. Kumar, Solid State Commun. 150 (2010) 1660–1664.
[9] L.Q. Zhang, Z.Z. Ye, B. Lu, J.G. Lu, J.Y. Huang, Y.Z. Zhang, Z. Xie, Solid State Commun. 155 (2013) 16–20.
[10] N.H. Hong, J. Sakai, N.T. Huong, N. Poirot, A. Ruyter, Phys. Rev. B 72 (2005) 045336.
[11] N.H. Hong, J. Sakai, V. Brizé, J. Phys.: Condens. Matter 19 (2007) 036219.
[12] J.L. MacManus-Driscoll, N. Khare, Y. Liu, M.E. Vickers, Adv. Mater. 19 (2007) 2925–2929.
[13] B.B. Straumal, A.A. Mazilkin, S.G. Protasova, A.A. Myatiev, P.B. Straumal, E. Goering, B. Baretzky, Thin Solid Films 520 (2011) 1192–1194.
[14] B.B. Straumal, A.A. Mazilkin, S.G. Protasova, P.B. Straumal, A.A. Myatiev, G. Schütz, E.J. Goering, T. Tietze, B. Baretzky, Philos. Mag. 93 (2013) 1371–1383.
[15] B.B. Straumal, S.G. Protasova, A.A. Mazilkin, B. Baretzky, A.A. Myatiev, P.B. Straumal, T. Tietze, G. Schütz, E. Goering, Mater. Lett. 71 (2012) 21–24.
[16] Y. Sato, T. Yamamoto, Y. Ikuhara, J. Am. Ceram. Soc. 90 (2007) 337–357.
[17] Y.-H. Li, Q. Xia, S.-K. Guo, Z.-Q. Ma, Y.-B. Gao, X.-G. Gong, S.-H. Wei, J. Appl. Phys. 118 (2015) 045708.
[18] G. Kresse, D. Joubert, Phys. Rev. B 59 (1999) 1758–1775.
[19] G. Kresse, J. Furthmüller, Comput. Mater. Sci. 6 (1996) 15–50.
[20] J.P. Perdew, Y. Wang, Phys. Rev. B 45 (1992) 13244–13249.
[21] S.L. Dudarev, G.A. Botton, S.Y. Savrasov, C.J. Humphreys, A.P. Sutton, Phys. Rev. B 57 (1998) 1505–1509.
[22] S. Lany, H. Raebiger, A. Zunger, Phys. Rev. B 77 (2008) 241201.
[23] S. Lany, A. Zunger, Phys. Rev. B 72 (2005) 035215.
[24] D.R. Lide, CRC Handbook of Chemistry and Physics, 90th ed., CRC Press, Boca Raton, FL, USA, 2010.
[25] F. Oba, H. Ohta, Y. Sato, H. Hosono, T. Yamamoto, Y. Ikuhara, Phys. Rev. B 70 (2004) 125415.
[26] A. Walsh, J.L. Da Silva, S.H. Wei, Phys. Rev. Lett. 100 (2008) 256401.
[27] E.-Z. Liu, J.Z. Jiang, J. Appl. Phys. 107 (2010) 023909.
[28] P. Gopal, N.A. Spaldin, Phys. Rev. B 74 (2006) 094418.
[29] T. Dietl, Science 287 (2000) 1019–1022.
[30] C. Song, K.W. Geng, F. Zeng, X.B. Wang, Y.X. Shen, F. Pan, Y.N. Xie, T. Liu, H.T. Zhou, Z. Fan, Phys. Rev. B 73 (2006) 024405.
[31] C. Song, F. Zeng, K.W. Geng, X.J. Liu, F. Pan, B. He, W.S. Yan, Phys. Rev. B 76 (2007) 045215.
[32] A.J. Behan, A. Mokhtari, H.J. Blythe, D. Score, X.H. Xu, J.R. Neal, A.M. Fox, G.A. Gehring, Phys. Rev. Lett. 100 (2008) 047206.
[33] A. Dinia, G. Schmerber, V. Pierron-Bohnes, C. Mény, P. Panissod, E. Beaurepaire, J. Magn. Magn. Mater. 286 (2005) 37–40.